RSC Advances

ROYAL SOCIETY OF CHEMISTRY

www.rsc.org/advances

Graphical Abstract

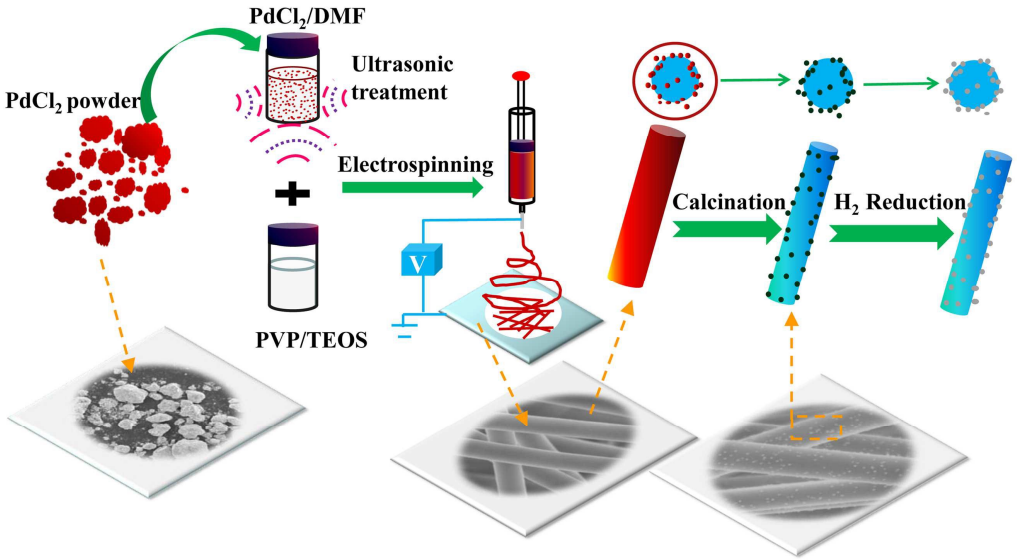

A new inorganic supported catalyst of silica (SiO_2)-supported palladium (Pd) nanofibers was successfully fabricated by the electrospinning followed by the calcination at high temperature and the reduction in H_2 atmosphere

RSC Advances

RSCPublishing

ARTICLE

Electrospinning of Palladium/Silica Nanofibers for Catalyst Applications

Shipeng Wen,[a,b] Meili Liang,[a,b] Rui Zou,[a] Zhoujun Wang[a], Dongmei Yue*[a] and Li Liu*[b,c]

Cite this: DOI: 10.1039/x0xx00000x

Received ooth January 2012,
Accepted ooth January 2012

DOI: 10.1039/x0xx00000x

www.rsc.org/

Supported catalyst is an increasingly popular research area because supported catalysts are highly efficient and the catalyst particles can be recovered. In this study, a new silica-supported palladium (Pd/SiO_2) nanofiber catalyst was developed. Pd/SiO_2 nanofibers were prepared by the electrospinning of a solution mixture of poly(vinyl pyrrolidone) (PVP), TEOS gel, and $PdCl_2$ nanoparticles, followed by the calcination of $PdCl_2$/PVP/TEOS nanofibers at a high temperature and the reduction of PdO/SiO_2 nanofibers in a H_2 atmosphere. The results showed that the prepared Pd/SiO_2 nanofibers had an average diameter of 500 nm. Pd nanoparticles with a diameter of 20-30 nm were uniformly dispersed on the surface of SiO_2 nanofibers. The composite nanofibers had high Brunner-Emmett-Teller (BET) specific surface area. The hydrogenation reaction for acrylic acid showed that the hydrogenation efficiency was 93.48% in the presence of 0.1 g of Pd/SiO_2 nanofibers. These nanofibers could be easily recycled. These features make the Pd/SiO_2 nanofibers promising in a wide range of applications in the catalyst industry.

Introduction

Rare-metals, such as palladium,[1, 2] rhodium,[3, 4] and platinum,[5, 6] are always the research focus in the catalyst field because of their high catalytic activity in hydrogenation, oxidation, and hydrogenolysis.[7-11] In recent decades, researchers have devoted to increasing the catalytic activity and catalytic efficiency of these rare metals because these metals are really expensive and very difficult to reclaim. For instance, rare-metal nanoparticles have shown much higher catalytic activity than microparticles.[12] However, the nanoparticles are quite difficult to reclaim from the reaction solution because of their small size. The waste solution poses a great pollution on the environment without reclamation of rare-metals. Supported catalysts have attracted more and more attention because they can provide high catalytic activity and a way to reclaim the catalyst.[13, 14] A supported catalyst is composed of rare-metal nanoparticles and a matrix such as a molecular sieve,[15] carbon nanotubes,[16] carbon fibers,[17, 18] and silica.[19] The nanoparticles have a fine dispersion in the solution, and subsequently enhance the catalytic efficiency. For instance, Bhat et al.[20] prepared zeolite-Y-supported rhodium particle catalysts by ion exchange starting from an aqueous solution of $[Rh[(NH_3)_5Cl]Cl_2 \cdot 6H_2O]$. The high dispersion (near 100 %) of rhodium particles with a diameter of 4 nm resulted in 90 mol% conversion of CO_2+CH_4 to $CO+H_2$ at a low Rh loading of 0.5 to 0.93 %. This supported catalyst exhibited extraordinary stability and high activity and selectivity. Deng et al.[21] reported the catalytic hydrodechlorination (HDC) of 4-chlorophenol (4-CP) over a multiwalled-carbon-nanotubes (MWCNTs)-supported palladium catalyst by using the impregnation method. The results showed that the as-prepared catalyst Pd/MWCNTs exhibited higher stability for the HDC of 4-CP than conventional catalysts because of the highly dispersed Pd nanoparticles on the MWCNT support and the interaction between the support and metal actives.

Electrospinning as an effective and universal method to prepare nanofibers has attracted increasing attention in recent years.[22-25] The electrospun fibers show excellent features such as nanosize, mesoporous nanostructure, large specific surface area, and controllable morphology.[26-28] These features make the nanofibers a promising and attractive candidcate for catalyst support because the nanofibers can provide more active sites for the catalyst to improve the catalytic efficiency. Various nanofiber-supported catalyst have been prepared by electrospinning. For instance, Guo et al.[29] prepared Pd nanoparticle/poly(vinyl pyrrolidone) (PVP) nanofiber membranes by electrospinning. PVP served as the protecting agent as well as the support for the Pd nanoparticles. The results showed that Pd NPs/PVP nanofiber catalysts possessed high-activity, improved selectivity and yield, the conversion rate of paratoluidine was 74.36

%. Fang et al.[30] prepared polyethyleneimine (PEI)/polyvinyl alcohol (PVA) nanofibers by electrospinning and gold nanoparticles (Au NPs) were immobilized on the surface of nanofibers with impregnation method. The results showed that the Au NPs/PEI/PVA nanofibers with an average diameter of 490 nm were able to catalyze the reaction of 4-nitrophenol to 4-aminophenol with an efficiency approaching 97 % within 36 min.

According to the above reports, most electrospun-fiber-supported catalysts used a polymer as the support. However, most polymer matrixes are solvent- and temperature-sensitive, restricting the catalytic effect. Therefore, the use of inorganic nanofibers as the support is a good choice. In our previous study, SiO_2 nanofibers with a diameter of 400-500 nm were fabricated successfully by electrospinning in combination with the sol-gel process. The SiO_2 nanofibers have many advantages such as non-toxicity and easy surface modification. Furthermore, SiO_2 nanofibers are stable, difficult to destroy in solvents, and easy to recycle. Hence, SiO_2 nanofibers are suitable for use as catalyst support.

Pd as a common catalyst with high catalytic activity is often used for hydrogenation, oxidation, and hydrogenolysis. However, Pd particles are very expensive and difficult to recycle. In this study, Pd/SiO_2 nanofibers were fabricated by a combination of electrospinning, calcination, and reduction. The SiO_2-supported catalyst nanofibers showed a diameter of about 500 nm, and the Pd nanoparticles with a size of 20-30 nm were evenly and firmly attached on the surface of the SiO_2 nanofibers. The specific surface area of the Pd/SiO_2 nanofibers was as high as 350-400 m^2/g. The catalytic hydrogenation of acrylic acid showed that the conversion reached 93.48 % in the presence of this novel Pd/SiO_2 nanofiber catalyst.

Experimental

Materials

Tetraethyl orthosilicate (TEOS) and poly(vinyl pyrrolidone) (PVP, Mw=130000) were purchased from Sigma Aldrich Co., Ltd. N,N-dimethyformamide (DMF, AR) and dimethylsulfoxide (DMSO, AR) were purchased from Beijing Eastern Chemical Company. Hydrochloric acid solution (37.5 v/v%) and ethanol (AR) were purchased from Beijing Chemical Company. Palladium chloride ($PdCl_2$, Pd≥59.50 %) particles were purchased from Shanghai Jiuling Company.

Preparation of Pd/SiO_2 composite nanofibers

The preparation of Pd/SiO_2 composite nanofibers is shown in Fig.1. First, 5.2 g of TEOS, 1.5 g of ethanol, and 1.0 g of hydrochloric acid solution were mixed under stirring for 12 h at room temperature to form solution (I). Second, 1.0 g of PVP powder was dissolved in a mixture of solvents composed of 4.0 g of DMF and 2.0 g of DMSO. The mixture was stirred continuously for 12 h to form a homogeneous and transparent solution (II). Third, $PdCl_2$ particles and 0.2 g of dispersant PVP were dispersed in 2.0 g of DMF in a sealed container. The mixture solution was followed by ultrasonication for 2 h to prepare solution (III). Finally, the above three different solutions were mixed under magnet stirring for 2 h. This final mixture solution was ready for electropinning. A series of mixture solutions for electrospinning with different $PdCl_2$ loadings (0.1, 0.2, and 0.3 g) were prepared.

The electrospinning solution was placed in a plastic syringe. The electrospinning setup was composed of a syringe pump (KDS-200), high voltage power supply (BGG6-351, High Voltage Technology Institute, Bemi Co., Ltd., China) and rotating drum (5 inches in diameter). The voltage was 15 kV. The feed rate was 1.0 ml/h. The rotational speed of the drum was 200-300 rpm/min, and the distance between the needle tip and the drum was 20 cm. The electrospun $PdCl_2$/PVP/TEOS nanofiber membrane was collected on an Al foil.

The electrospun nanofibers were calcinated in a Heavy Duty Tube Furnace (Lindberg 54453) first at 325 °C for 6 h and then at 800 °C for 1 h to remove the organic components.[31] During the calcination, the $PdCl_2$ nanoparticles were oxidized into PdO. Thereafter, the PdO/SiO_2 nanofibers were further reduced into Pd/SiO_2 nanofibers in a H_2 atmosphere at 70 °C. Finally, the Pd/SiO_2 nanofibers with 2.34, 5.15, and 8.52 wt.% of Pd nanoparticles were obtained.

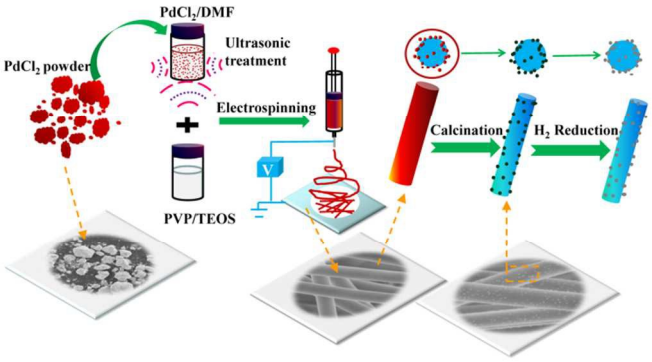

Fig. 1 Schematic for preparation of Pd/SiO_2 composite nanofibers

Hydrogenation and Measurement

25 mL of acrylic acid solution and 0.1 g of Pd/SiO_2 nanofibers containing 5.15 wt.% Pd were placed into a 100 mL autoclave. The autoclave was flushed three times with H_2 and N_2 to remove air before being heated to the reaction temperature of 70 °C. The reaction was initiated by flushing H_2 to 2.5 MPa under stirring at 500 rpm. After the hydrogenation, the catalyst was removed from the hydrogenated acrylic acid solution by filtration. For comparison purposes, the hydrogenation was catalyzed according to the above procedure, but with the Pd/SiO_2 nanofibers replaced by 0.00515 g of Pd powder. After hydrogenation, the Pd/SiO_2 nanofiber were filtered from reaction solution and washed with distilled water several times by centrifugal machine, and then dried under vacuum at 60 °C for 12 h.

Characterizations

The surface morphologies and the average diameters of the nanofibers before and after calcination were examined by scanning electron microscopy (SEM, Hitachi S-4800) and transmission electron microscopy (TEM, Hitachi H-800). The element contents of the nanofibers before and after calcination were determined by

energy dispersive X-ray spectroscopy (EDS, Genesis 307). Thermal gravimetric analysis (TGA, Mettler Toledo TGA/DSC/1100SF) was employed to evaluate the weight loss of the samples in air at a heating rate of 10 °C/min. X-ray photoelectron spectroscopy (XPS, Escalab 250) was used to determine the chemical composition and oxidation state of the Pd nanoparticles before and after calcination as well as reduction. The crystal structure of nanofibers was confirmed by X-ray diffraction (XRD, Bruker D8 Advance). The specific surface areas, pore volumes, and pore size of the Pd/SiO_2 nanofibers were determined based on N_2 adsorption−desorption isotherms measured on a Micromeritics ASAP 2020M analyzer. The hydrogenation efficiencies of the initial acrylic acid solution and hydrogenated reaction mixtures at different reaction times (t=1.5 h, 3 h, and 5 h) were determined by nuclear magnetic resonance (NMR, AV600) and the following equation:

$$HD = (1 - C_{c=c}/C_{c=c,0}) \times 100\%, \quad (1)$$

where $C_{c=c,0}$ and $C_{c=c}$ are the hydrogen concentrations at time zero and time t, respectively.

Results and discussion

The precursor nanofibers containing $PdCl_2$, PVP, and SiO_2 have a smooth surface and a diameter of about 700 nm, as shown in Fig. 2(A). SiO_2 existed in the precursor nanofibers as a Si-O-Si gel, which was formed in the electrospinning solution. The TEM image in Fig. 2(B) shows that the composite nanofibers have a core-sheath structure. The core and sheath layers are mainly composed of TEOS gel and PVP, respectively. This special structure is mainly attributed to the poor incompatibility and the phase separation between the SiO_2 gel and PVP.[32]

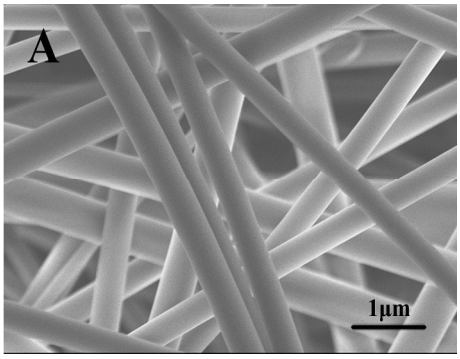

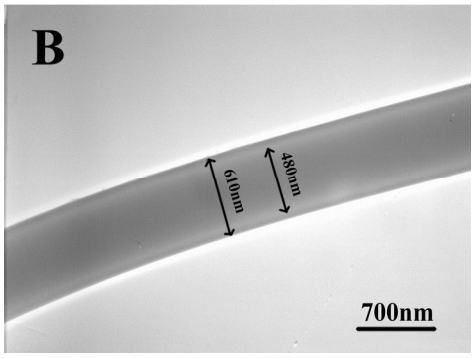

Fig. 2 (A) SEM image and (B) TEM image of $PdCl_2$/PVP/SiO_2 composite nanofibers with 5.15 wt.% of Pd

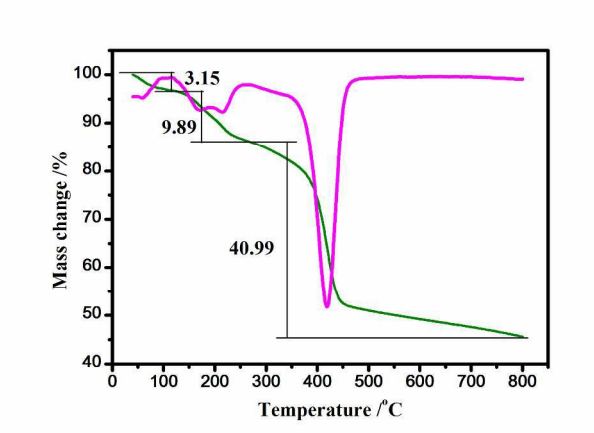

Fig. 3 TG and DTG curves of $PdCl_2$/PVP/TEOS composite fibers

To obtain inorganic SiO_2-fibers-supported Pd nanoparticles, PVP and other organic phases in the precursor nanofibers should be removed by calcination at high temperatures. The TG and DTG curves of the precursor fibers in Fig. 3 shows four steps and a total loss of 54.04 wt.%. The first weight-loss of 3.15 wt.% at 59 °C is due to the evaporation of solvents (ethanol, DMF, and H_2O) remaining in the precursor fibers. The second significant weight-loss of 9.89 wt.% at 218 °C is assigned to the decomposition of the side chains of PVP. The third weight-loss of 40.99 wt.% in the range of 300-500 °C is assigned to the complete decomposition of PVP[33] and the release of the water formed in the condensation of silanols in the silica gels[34] and the conversion of the metal precursor ($PdCl_2$) into metal oxide (PdO).[35] Hence, the fibers obtained above 600 °C have been converted into silica-fiber-supported metal oxide (PdO).

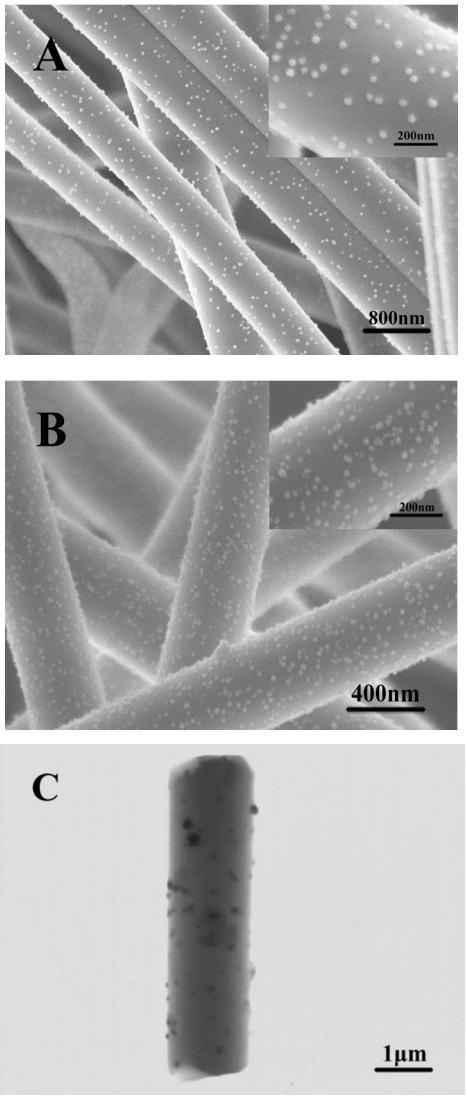

Fig. 4 PdO/SiO_2 composite nanofibers after calcination: (A) SEM image of fibers with 2.34 wt.% of Pd, (B) SEM image of fibers with 5.15 wt.% of Pd and (C) TEM image of fiber with 5.15 wt% of Pd

Fig. 4 shows the morphologies of PdO/SiO_2 composite nanofibers. The SEM images in Fig. 4(A) and 4(B) indicate that the average diameter of PdO/SiO_2 nanofibers is about 500 nm (a decrease from that of $PdCl_2/PVP/SiO_2$ nanofibers). This decrease in diameter is attributed to the pyrolysis of organic components during the calcination process. Fig. 4B and 4C both show that PdO nanoparticles with a diameter of 20-30 nm are dispersed uniformly on the surface of silica nanofibers, although $PdCl_2$ nanoparticles were dispersed both inside and on the surface of the nanofibers during the electrospinning. Additionally, the amount of PdO nanoparticles on the surface of the PdO/SiO_2 nanofibers and the roughness of the PdO/SiO_2 nanofibers increase with the increase of the amount of $PdCl_2$ nanoparticles. The rough surface of the nanofibers is beneficial to the increase in the catalytic efficiency of the composite fibers.

Table 1 EDS results of PdO/SiO_2 composite nanofibers containing 5.15 wt% of Pd

Content /wt%	C	O	Si	N	S	Cl	Pd
Before pyrolysis	30.15	40.21	17.22	9.36	1.95	0.56	0.56
After pyrolysis	7.01	54.14	34.89	0	0	0	3.95

The element contents of the fibers before and after calcination were analyzed by EDS tests. Table1 indicates the existence of C, O, Si, N, S, Cl, and Pd in the $PdCl_2/PVP/TEOS$ fibers before calcinations. After calcination, the content of C decreases from 30.15 to 7.01 wt%, while N, S, and Cl are not detected. This change indicates that PVP and other organic phases from the solvents degrade during the calcination. Additionally, the disappearance of Cl confirms that the $PdCl_2$ nanoparticles have been converted into PdO nanoparticles. Because PdO nanoparticles have no catalytic activity for hydrogenation, the PdO/SiO_2 nanofibers need to be further reduced to Pd/SiO_2 nanofibers in a hydrogen atmosphere.

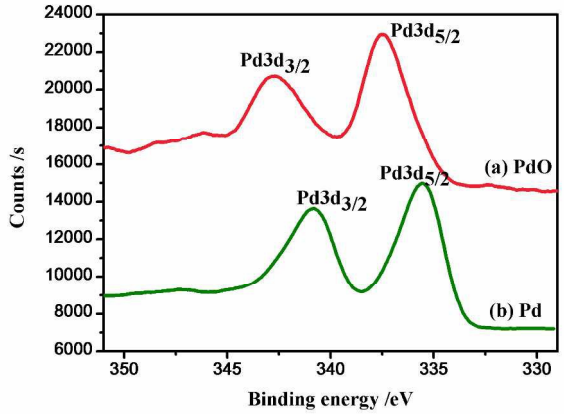

Fig.5 Pd3d XPS spectra of composite nanofibers before and after H_2 reduction

The XPS spectra in Fig. 5 show the variations of Pd binding energy for the composite fibers before and after H_2 reduction. In Fig. 5A, the peaks at 337.5 and 342.6 eV in curve (a) are attributed to the $Pd3d_{5/2}$ and $Pd3d_{3/2}$ of PdO[36, 37]. After H_2 reduction, the two peaks shift to 335.7 and 341.0 eV in curve (b)[38, 39]. These shifts confirm that the PdO nanoparticles in the nanofibers have been reduced to Pd nanoparticles.

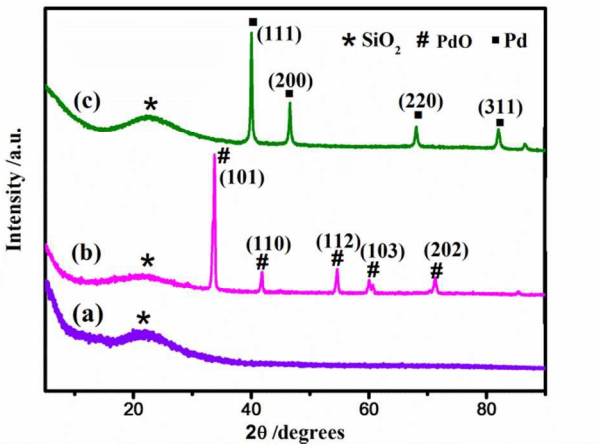

Fig. 6 XRD patterns of (a) SiO_2 nanofibers, (b) PdO/SiO_2 nanofibers, and (c) Pd/SiO_2 nanofibers

Fig. 6 shows the crystal structures of SiO_2 nanofibers, PdO/SiO_2 nanofibers, and Pd/SiO_2 nanofibers. In pattern (a) for the SiO_2 nanofibers, the broad peak at 2θ=22° indicates that the SiO_2 nanofibers are amorphous. In pattern (b) for the PdO/SiO_2 nanofibers, the diffraction peaks at about 2θ=33.9°, 41.9°, 54.8°, 60.2°, and 71° are indexed to PdO (101), PdO (110), PdO (112), PdO (103), and PdO (211), respectively (JCPDS No.6-515, No.85-624). The sizes of PdO nanoparticles calculated by the Scherrer equation[40] are about 17.92 nm (101), 21.83 nm (110), and 21.03 nm (112). In pattern (c) for the Pd/SiO_2 nanofibers, the diffraction peaks at 40.1°, 46.7°, 68.1°, and 81.68° are attributed to the (111),(200),(220), and (311) planes of Pd, respectively, indicating the face-centered cubic crystal structure of Pd nanoparticles (JCPDS, No. 65-6174). The obtained crystalline sizes are 22.03 nm (111), 20.78 nm (200), and 20.78 nm (220). These sizes of the Pd nanoparticles are consistent with the results obtained by SEM observations. No diffraction peaks for PdO in Fig. 6(c) indicate that the PdO nanoparticles in the nanofibers have been reduced to Pd nanoparticles after H_2 reduction. This result is consistent with that obtained in XPS test. The diffraction peak of SiO_2 is also detected in both pattern (b) and pattern (c), indicating that Pd nanoparticles are immobilized on the SiO_2 nanofibers.

Table 2 BET specific surface area of $PdCl_2$ powder and Pd/SiO_2 nanofibers

Sample	$PdCl_2$ powder	Pd/SiO_2 nanofibers		
		2.34 wt.% of Pd	5.15 wt.% of Pd	8.52 wt.% of Pd
BET /m^2/g	26.57	348.83	374.92	401.28

The BET specific surface area is an important parameter for catalysts. As shown in Table 2, the BET specific surface area of $PdCl_2$ is about 26.57 m^2/g. Our previous study[41] showed that solid SiO_2 nanofibers without pores had a BET specific surface area of 4.14 m^2/g. However, the Pd/SiO_2 nanofibers with different Pd contents show much higher BET specific surface area than $PdCl_2$ powder and solid SiO_2 nanofibers. It is speculated that the high BET specific surface area on the Pd/SiO_2 nanofibers is attributed to the bumpy surface and some pores on the surface of the fiber.[42] To further verify the existence of pores on the surface of the Pd/SiO_2 nanofibers, N_2 adsorption-desorption isotherm of Pd/SiO_2 nanofibers with 5.15 wt.% of Pd is shown in Fig. 7. The adsorption–desorption curve exhibits a type IV profile according to the IUPAC classification. The shape of hysteresis loop (type H4) formed by capillary condensation indicates that some mesopores exist in the slits of the fibers. The slits may come from the interface gap between nanoparticles and SiO_2 nanofibers. The BET surface area and volume of the Pd/SiO_2 nanofibers catalyst is 374.92 m^2/g and 0.3 cm^3/g, respectively. The pore size is 3.8 nm within the mesopore range (2–50 nm). This mesoporous structure is beneficial to the increase in catalytic efficiency of the fibers because the molecules have more opportunity to contact the Pd nanoparticles during the reaction.

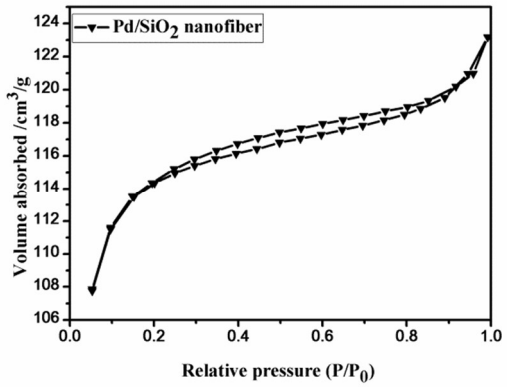

Fig.7 N_2 adsorption-desorption isotherms of Pd/SiO_2 nanofibers with 5.15 wt.% of Pd

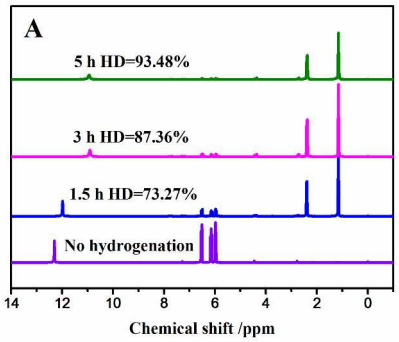

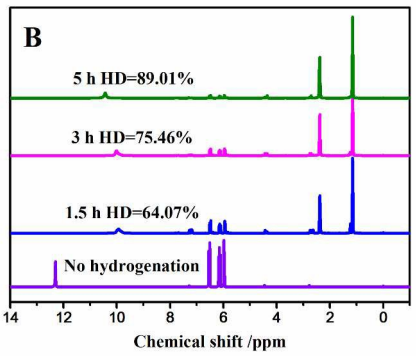

Fig. 8 NMR spectra of acrylic acid hydrogenated by (A) Pd/SiO_2 nanofibers with 5.15 wt.% of Pd and (B) Pd powder

Palladium as a highly efficient catalyst is mainly used in hydrogenation, oxidation, and hydrogenolysis. In this study, a Pd/SiO_2 nanofiber catalyst was used for the hydrogenation of acrylic acid. The catalytic effect was characterized by NMR, and the results are shown in Fig. 8. With the increase of reaction time, the intensity of the peak between 5.5-7.0 ppm for the double bond gradually decreases, while the intensity of the alkyl peak between 1.0-2.5 ppm increases. The proton peak of -COOH also moves to a lower ppm value. These results show that acrylic acid is gradually converted into propionic acid. The degree of hydrogenation of acrylic acid reaches 93.48 % in the presence of 0.1 g of Pd/SiO_2 nanofibers at a reaction time of about 5 h. This catalytic efficiency is even higher than that (89.01%) of Pd powder at the same catalyst content. The high catalytic efficiency of Pd/SiO_2 nanofibers is attributed to the fine dispersion and the high specific surface area of Pd particles on the surface of SiO_2 fibers.

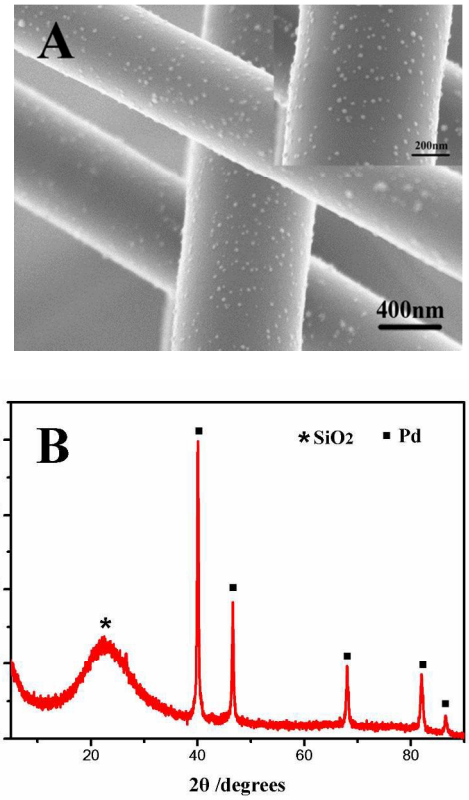

Fig.9 (A) SEM image and (B) XRD pattern of Pd/SiO_2 nanofibers after hydrogenation

After hydrogenation, Pd/SiO_2 nanofiber catalysts were reclaimed, followed by filtering and drying. Fig. 9(A) shows the morphologies of Pd/SiO_2 nanofibers after hydrogenation. Pd/SiO_2 nanofibers have the average diameter of 500 nm, and Pd nanoparticles with a diameter of 20-30 nm are still dispersed uniformly on the surface of the nanofibers, indicating that the morphologies of Pd/SiO_2 nanofibers have no change compared with those before reaction. Fig. 9(B) presents XRD pattern of Pd/SiO_2 nanofiber catalysts after reaction. The patterns in Fig. 9(B) are consistent with those before reaction in Fig. 6(c). According to Scherrer equation, the average crystalline size of Pd in the nanofibers was calculated to be 20.4 nm, which is similar with that before reaction. The above results show that the structure of Pd/SiO_2 nanofibers did not change during the hydrogenation.

Conclusions

Pd/SiO_2 composite nanofibers with an average diameter of 500 nm were prepared by electrospinning in combination with a sol-gel reaction. The results indicated that Pd nanoparticles with the diameter of 20-30 nm were evenly dispersed and firmly attached on the surface of SiO_2 nanofibers. The Pd/SiO_2 nanofibers showed much higher BET specific surface area than Pd powder. The degree of hydrogenation (93.48%) for acrylic acid catalyzed by the Pd/SiO_2 nanofibers was higher than that for acrylic acid catalyzed by Pd powder at the same catalyst content. The Pd/SiO_2 catalyst can be easily recycled, showing great application potential in the catalyst industry.

Acknowledgements

This study was supported by the National Basic Research Program of China (2015CB654700(2015CB674705)), the National Natural Science Foundation of China (51103005 and 21403012), the Beijing Natural Science Foundation (2144053), the Fundamental Research Funds for the Central Universities in China (JD1407 and 1404), the Beijing Higher Education Young Elite Teacher Project (YETP0493), and the Program of Beijing Excellent Talents (2013D009016000003).

Notes and references

[a]State Key Laboratory of Organic-Inorganic Composites, Beijing University of Chemical Technology, Beijing 100029, China
[b]Beijing Engineering Research Center of Advanced Elastomers, Beijing University of Chemical Technology, Beijing 100029, China
[c]State Key Laboratory of Chemical Resource Engineering, Beijing University of Chemical Technology, Beijing 100029, China

1 H. Q. Guo, S. Q. Tao, *IEEE Sensors J.*, 2007, **7**, 323-328.
2 B. C. Liu, Q. Wang, S. L. Yu, P. Jing, L. X. Liu, G. G. Xu, J. Zhang, *Nanoscale*, 2014, **6**, 11887-11897.
3 Q. S. Zhao, D. F. Chen, Y. Li, G. L. Zhang, F. B. Zhang, X. B. Fan, *Nanoscale*, 2013, **5**, 882-885.
4 I. S. Park, M. S. Kwon, N. Kim, J. S. Lee, K. Y. Kang, J. Park, *Chem. Commun.*, 2005, (45) 5667-5669.
5 R. X. Wang, J. J. Fan, Y. J. Fan, J. P. Zhong, L. Wang, S.G. Sun, X.C. Shen, *Nanoscale*, 2014, **6**, 14999-15007.
6 H. J. Tang, H. Y. Sun, D. R. Chen, X. L. Jiao, *Mater. Lett.*, 2012, **77**, 7-9.
7 A. B. Chen, Y. L. Li, J. Z. Chen, G. Y. Zhao, L. L. Ma, Y. F. Yu, *Chempluschem*, 2013, **78**, 1370-1378.
8 Q. H. Guo, J. S. Huang, T. Y. You, *Chinese J. Anal. Chem.*, 2013, **41**, 210-214.
9 H. Bernas, A. J. Plomp, J. H. Bitter, D. Y. Murzin, *Catal. Lett.*, 2008, **125**, 8-13.

10 M. J. Jacinto, P. K. Kiyohara, S. H. Masunaga, R. F. Jardim, L. M. Rossi, *Appl. Catal. A-Gen*., 2008, **338**, 52-57.
11 E. P. Maris, R. J. Davis, *J. Catal.*, 2007, **249**, 328-337.
12 B. D. Summ, N. I. Ivanova, *Russ. Chem.Rev.*, 2000, **69**, 911.
13 W. Shi, W.S. Lu, L. Jiang, *J. Colloid Interface Sci.*, 2009, **340**, 291-297.
14 H. G. Kang, Y. H. Zhu, Y. J. Jing, X. L. Yang, C. Z Li, *Colloids Surf. A*, 2010, **356**, 120-125.
15 Y. H. Hsien, C. F. Chang, Y. H. Chen, S. Cheng, *Appl. Catal. B-Environ.*, 2001, **31**, 241-249.
16 V. Tzitzios, V. Georgakilas, E. Oikonomou, M. Karakassides, D. Petridis, *Carbon*, 2006, **44**, 848-853.
17 P. Zhang, C. L. Shao, Z. Y. Zhang, M. Y. Zhang, J. B. Mu, Z. C. Guo, Y. C. Liu, *Nanoscale*, 2011, **3**, 3357-3363.
18 Y. J. Ou, W. W. Si, G. Yu, L. L. Tang, J. Zhang, Q. Z. Dong, *J. Alloys Compd.*, 2013, **569**, 130-135.
19 S. Duhan, V. K. Tomer, A. K. Sharma,B. S. Dehiya, *J. Alloys Compd.*, 2014, **583**, 550-553.
20 R. Bhat,W. Sachtler, *Appl. Catal. A-Gen.*, 1997, **150**, 279-296.
21 H. Y. Deng, G. Y. Fan, Y. H. Wang, *Synth. React. Inorg. Met.-Org. Chem.*, 2014, **44**, 1306-1311.
22 H. W. Tong, B. R. Mutlu, L. P. Wackett, A. Aksan, *Mater. Lett.*, 2013, **111**, 234-237.
23 A. Greiner, J. H. Wendorff, *Angew. Chem. Int. Ed.*, 2007, **46**, 5670-5703.
24 H. Y. He, J. Wang, X. Li, X. W. Zhang, W. J. Weng, G. R. Han, *Mater. Lett.*, 2013, **94**, 100-103.
25 M. G. Zhao, X. C. Wang, L. L. Ning, H. He, J. F. Jia, L. W. Zhang, X. J. Li, *J. Alloys Compd.*, 2010, **507**, 97-100.
26 H. Y. Guan, W. Zhou, S. W. Fu, C. L. Shao, Y. C. Liu, *J. Phys. Chem. Solids*, 2009, **70**, 1374-1377.
27 H. G. Zhao, C. W. Jia, H. G. Duan, Z. W. Sun, X. M. Wang, E. Q. Xie, *J. Alloys Compd.*, 2008, **455**, 497-500.
28 Y. Bao, Q. A. N. Luu, Y. Zhao, H. Fong, P. S. May, C. Jiang, *Nanoscale*, 2012, **4**, 7369-7375.
29 L. P. Guo, J. Bai, C. P. Li, Q. R. Meng, H. O. Liang, W. Y. Sun, H. Q. Li, H. Liu, *Appl. Surf. Sci*., 2013, **283**, 107-114.
30 X. Fang, H. Ma, S. L. Xiao, M. W. Shen, R. Guo, X. Y. Cao, X. Y. Shi, *J. Mater. Chem.*, 2011, **21**, 4493-4501.
31 T. H. San, W. R. W. Daud, A. A. H. Kadhum, A. B. Mohamad, S. K. Kamarudin, L. K. Shyuan, E. H. Majlan, *AIP Conf. Proc.*, 2012, **1455**,109-113.
32 W. Wang, J. Y. Zhou, S. S. Zhang, J. Song, H.G. Duan, M. Zhou, C. S. Gong, Z. Bao, B. G. Lu, X. D. Li, *J. Mater. Chem.*, 2010, **20**, 9068-9072.
33 X. Wang, H. Q. Fan, P. R. Ren, H. W. Yu, J. Li, *Mater. Res. Bull.*, 2012, **47**, 1734-1739.
34 Y. Y. Zhao, H. Y. Wang, X. F. Lu, X. Li, Y. Yang, C. Wang, *Mater. Lett.*, 2008, **62**, 143-146.
35 S. Swaminathan, G. Chase, *Electrospinning of Metal Doped Alumina Nanofibers for Catalyst Applications*, in *Nanofibers-Production, Properties and Functional Applications,* T. Lin, Ed., *InTech*, 2011.
36 H. Yang, N. Alonso-Vante, C. Lamy, D. L. Akins, *J. Electrochem. Soc.*, 2005, **152**, A704-A709.
37 T. Ramulifho, K. I. Ozoemena, R. M. Modibedi, C. J. Jafta, M. K. Mathe, *Electrochim. Acta*, 2012, **59**, 310-320.
38 M. L. Wang, W. W. Liu, C. D. Huang, *Int. J. Hydrogen Energy*, 2009, **34**, 2758-2764.
39 F. X. Yin, S. F. Ji, P. Y. Wu, F. Z. Zhao, C. Y. Li, *J. Catal*., 2008, **257**, 108-116.
40 H. Z. Huang, *Nanomaterials Analysis, Chemical Industry Press: Beijing*, 2003.
41 S. P. Wen, L. Liu, L. F. Zhang, Q. Chen, L. Q. Zhang, H. Fong, *Mater. Lett.*, 2010, **64**, 1517-1520.
42 M. Bognitzki, W. Czado, T. Frese, A. Schaper, M. Hellwig, M. Steinhart, A. Greiner, J. H. Wendorff, *Adv. Mater.*, 2001, **13**, 70-72.